The Effect of Using $H_4P_2O_7$ as Phosphorus Source for Synthesizing Vanadyl Pyrophosphate Catalysts

Y.H. Taufiq-Yap*, A. Raslan and R. Irmawati

Department of Chemistry, Universiti Putra Malaysia, 43400 Serdang, Selangor, Malaysia

Abstract

Vanadyl pyrophosphate $(VO)_2P_2O_7$ catalysts synthesized via $VOPO_4{\cdot}2H_2O$ were investigated by using BET surface area measurement, X-ray Diffraction (XRD), Scanning Electron Microscope (SEM), and Temperature-Programmed Techniques (TPD and TPRS). H_3PO_4 and $H_4P_2O_7$ were used as the phosphorus source. Only pyrophosphate phase was observed for both final catalysts after 75 hours of calcination in a reaction flow of *n*-butane/air mixture (0.75% *n*-butane/air). However, catalyst derived from $H_4P_2O_7$ based preparation (denoted VPD_{pyro}) exhibit better crystallinity and slightly higher BET surface area compared to the H_3PO_4 based preparation (denoted VPD_{ortho}). The nature of the oxidants for both catalysts was investigated by O_2-TPD. For VPD_{pyro}, TPD showed an oxygen peak maximum at 986 K and a shoulder at 1003 K, whereas for VPD_{ortho}, the oxygen was desorbed as two peaks maxima at 966 and 994 K. The total amount of oxygen desorbed thermally from VPD_{pyro} (3.60×10^{20} atom$\times g^{-1}$) is higher than that obtained for VPD_{ortho} (3.07×10^{20} atom$\times g^{-1}$). VPD_{pyro} displayed a slightly improved activity and selectivity for *n*-butane oxidation. A proper amount of V^{5+} species may have an effect on the enhancement of the catalytic activity.

Introduction

Vanadyl pyrophosphate, $(VO)_2P_2O_7$ catalysts currently are the most active phase to transform the only alkane used commercially in selective oxidation process from *n*-butane to maleic anhydride (MA). Maleic anhydride is an important material for manufacturing unsaturated polyester resins, agricultural chemical, food additives, lubricating oil additives and pharmaceuticals [1].

Most of the studies reported that $(VO)_2P_2O_7$ was obtained from the precursor $VOHPO_4{\cdot}0.5H_2O$, by calcination in a reaction condition at 673 K. This precursor played an important role in the transformation of the final catalyst [2]. Preparation of the precursor is the key to obtain a high performance catalyst [3,4,5, 6]. The phosphorus sources employed for the synthesis of $VOHPO_4{\cdot}0.5H_2O$ also reported to give a strong influence in the synthesis of vanadium phosphate catalysts [3].

The purpose of this paper is to investigate the physico-chemical properties of the vanadyl pyrophosphate, $(VO)_2P_2O_7$ catalyst prepared by using two different sources of phosphorus *i.e.*: H_3PO_4 and $H_4P_2O_7$. The catalytic activity of these catalysts will also be reported.

Experimental

Catalysts Preparation

Via $VOPO_4{\cdot}2H_2O$ and $H_4P_2O_7$

V_2O_5 (15.0 g) and $H_4P_2O_7$ (69.9 g) mixture was refluxed in water for 4 hours. Then the resulting mixture (yellowish coloured) was recovered by centrifuged, following by filtration and washed with cold water. The solid obtained was then dried in air for 24 hours at 373 K and confirmed by XRD as $VOPO_4{\cdot}2H_2O$. This material was refluxed with isobutanol for 16 hours to obtain $VOHPO_4{\cdot}0.5H_2O$ precursor (denoted $Pyro_{pre.}$).

Via $VOPO_4{\cdot}2H_2O$ and H_3PO_4

$VOPO_4{\cdot}2H_2O$ was prepared by mixing V_2O_5 (15.0 g) with H_3PO_4 (90 mL). This mixture was refluxed in water for 16 hours. Then the resulting mixture (yellowish coloured) was recovered by filtration and

*corresponding author. E-mail: yap@fsas.upm.edu.my

Printed in Kazakhstan

washed with cold water and dried in air for 24 hours at 373 K. $VOPO_4{\cdot}2H_2O$ was then refluxed with isobutanol for 16 hours to obtain the $VOHPO_4{\cdot}0.5H_2O$ precursor (denoted as $Ortho_{pre}$).

These resulting precursors were then calcined in a flow of *n*-butane/air mixture (0.75% *n*-butane in air) for 75 hours at 673 K. The final catalysts were denoted VPD_{pyro} (using $H_4P_2O_7$) and VPD_{ortho} (using H_3PO_4).

Catalysts Characterization

The BET surface areas of the catalysts were measured by using nitrogen adsorption at 77 K. This was done by using ThermoFinnigan Sorptomatic Instrument model 1990.

The bulk average oxidation states of vanadium in the catalysts were determined by redox titration following the method of Niwa and Murakawi [7].

The X-ray diffraction (XRD) analyses were carried out using a Shimadzu diffractometer model XRD 6000 employing Cu K_α radiation to generate diffraction patterns from powder crystalline samples at ambient temperature.

SEM was done using a Quanta 200 ESEM FEG electron microscope.

Temperature Programmed Desorption (TPD) of O_2 analysis was done by using a ThermoFinnigan TPDRO 1110 apparatus utilizing a thermal conductivity detector (TCD).

Temperature Programmed Reaction Spectroscopy (TPRS) profile was obtained by passing an *n*-butane/He stream (2.0%, 101 kPa, 25 $cm^3{\times}min^{-1}$) over the catalyst (0.5 g) and raising the temperature from ambient to 1173 K at 5 $K{\times}min^{-1}$. This was done by using ThermoFinnigan TPDRO 1100 apparatus connected via a heated capillary to a quadrupole MS (Pfeiffer).

Results and Discussion

BET surface area measurement and redox titration

The BET surface area for VPD_{ortho} and VPD_{pyro} are 23.18 and 25.40 $m^2{\times}g^{-1}$, respectively. These values are higher compared to 12.0 $m^2{\times}g^{-1}$ as reported by Bartley *et al*. [3]. The average oxidation numbers of vanadium for both catalysts are given in Table 1. By using $H_4P_2O_7$ as the phosphorus source was found to decrease the average oxidation number from 4.26 to 4.18 *i.e.* a reduction of V^{5+} oxidation state from 26 to only 18%. This observation is similar to those reported by Bartley *et al*. [3].

Table 1

BET surface area, average vanadium valence and percentages of V^{4+} and V^{5+} oxidation states present for VPD_{ortho} and VPD_{pyro}

Catalysts	Specific surface area, ($m^2{\times}g^{-1}$)	V^{4+} (%)	V^{5+} (%)	Average oxidation state
VPD_{ortho}	23.18	74	26	4.26
VPD_{pyro}	25.40	82	18	4.18

X-ray Diffraction

The XRD pattern of the precursor, $Ortho_{pre}$ (Fig. 1) showed the characteristic peaks that matched perfectly with $VOHPO_4{\cdot}0.5H_2O$ with peaks appeared at 2θ = 15.6°, 27.0° and 30.4° which correspond to (001), (121) and (220) reflections, respectively. However, the usage of $H_4P_2O_7$ leads to the domination of reflection at 2θ = 30° which indexed to the (220) plane. This observation is similar to the previous report [3].

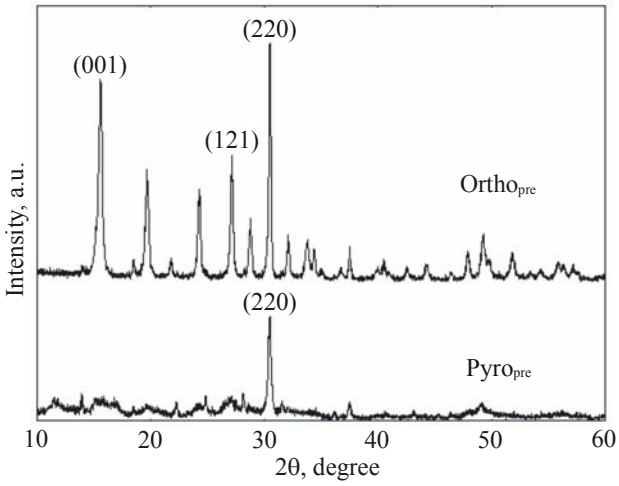

Fig. 1. XRD patterns of $Ortho_{pre}$ and $Pyro_{pre}$.

The XRD patterns for VPD_{ortho} and VPD_{pyro} catalysts shown in Fig. 2 were matched perfectly with the patterns of a pyrophosphate phase. The main peaks observed at 2θ = 23.0°, 28.5° and 29.9° which correspond to (020), (204) and (221) planes, respectively are more intense for the catalyst derived from $H_4P_2O_7$ compared to the catalyst prepared using H_3PO_4.

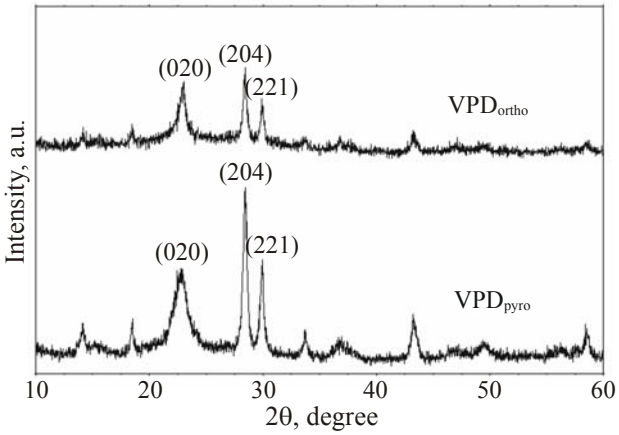

Fig. 2. XRD patterns of VPD_{ortho} and VPD_{pyro} catalyst.

Table 2 shows the line width of the (020) and (204) plane reflections. The parameter used to determined the crystallite size is the half width of the (020) peak. The line width increases with the decreasing size of the crystallite. The particle size of VPD_{ortho} at (020) and (204) were calculated by using Debye-Scherrer equation [8] as 151.9 and 97.7 Å, respectively. However, the particle size for VPD_{pyro} catalyst was decreased to 105.3 and 55.8 Å, respectively.

Table 2
XRD data for VPD_{ortho} and VPD_{pyro} catalysts

Catalysts	Line width (020), Å	Line width (204), Å	Thickness (020), Å	Thickness (204), Å
VPD_{ortho}	0.5400	0.8280	151.9	97.7
VPD_{pyro}	0.7809	1.4533	105.3	55.8

Scanning Electron Microscope

The surface morphologies of VPD_{ortho} and VPD_{pyro} are shown in Fig. 3. Both catalysts show a platelets structure which closely packed together forming a rosette-shape cluster. VPD_{ortho} showed a rosette type structure with a crystallite of uniformed sized however VPD_{pyro} catalyst showed an improper arrangement of rosette cluster with more isolated platelet.

Temperature-Programmed Desorption of Oxygen

The oxygen desorption spectra shown in Fig. 4 were obtained by pretreating the catalyst by heating them to 673 K in oxygen flow (1 bar, 25 $cm^3 \times min^{-1}$), holding them under that stream for 1 hour before cooling them to ambient temperature. Then the flow was switched to helium and the temperature was

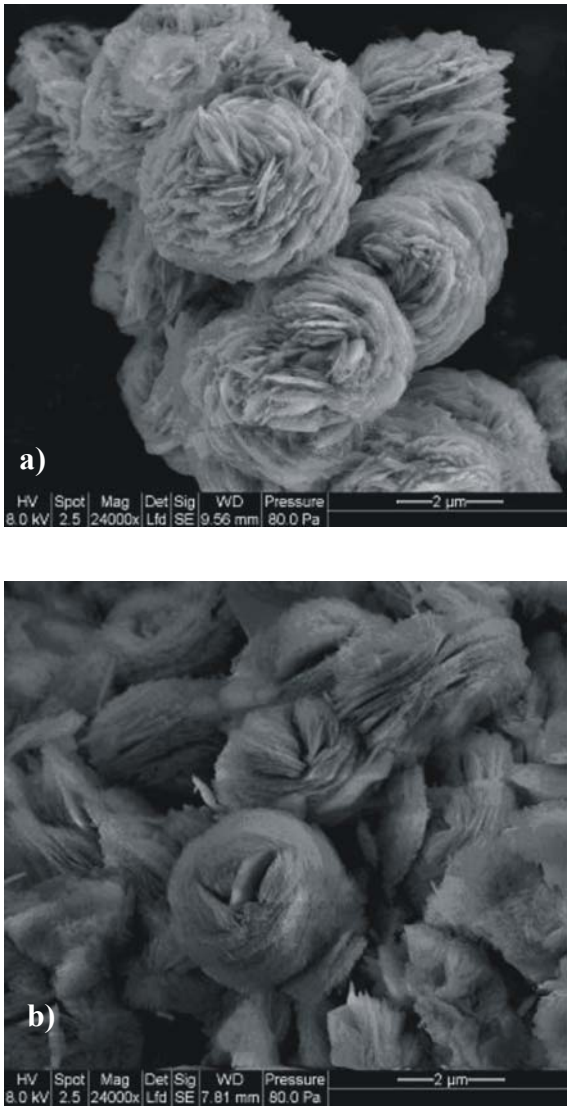

Fig. 3. (a) – SEM micrograph for VPD_{ortho}; (b) – SEM micrograph for VPD_{pyro}.

raised to 1173 K following the conductivity of oxygen by a thermal conductivity detector (TCD).

VPD_{ortho} gave two overlapped peaks at 966 and 994 K, whereas VPD_{pyro} also gave two desorption peaks maxima at 986 and 1003 K. There are no desorption peaks for oxygen in the temperature range from 300 to 850 K which correspond to the specific site for chemisorbed molecular oxygen. The total amount of oxygen desorbed from the VPD_{ortho} is 3.07×10^{20} atom$\times g^{-1}$ (Table 3). The usage of $H_4P_2O_7$ slightly increased the amount to 3.62×10^{20} atom$\times g^{-1}$ *i.e.*, an increment of ~15% of the total oxygen desorbed for VPD_{pyro}. These are the lattice oxygen which also has been observed earlier and showed 100% selectivity towards partial oxidation of C_4 hydrocarbons [9].

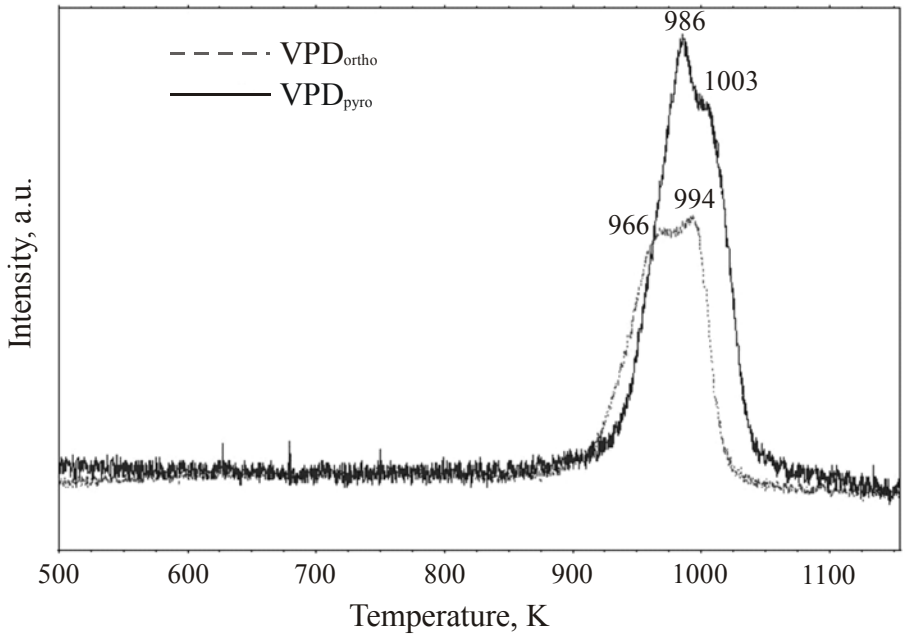

Fig. 4. O_2-TPD spectra of VPD_{ortho} and VPD_{pyro} catalysts.

Table 3
O_2-TPD data of VPD_{ortho} and VPD_{pyro} catalysts

Catalysts[a] (peaks)	T_{max}, (K)	Oxygen atom desorbed from the catalyst		Coverage ($atom \times cm^{-2}$)	Monolayers of oxygen removed[b]
		($mol \times g^{-1}$)	($atom \times g^{-1}$)		
VPD_{ortho}					
1	966	3.01×10^{-4}	1.82×10^{20}	7.85×10^{14}	1.1
2	994	2.08×10^{-4}	1.25×10^{20}	5.39×10^{14}	0.8
Total oxygen removed		5.09×10^{-4}	3.07×10^{20}	1.32×10^{15}	1.9
VPD_{pyro}					
1	986	3.39×10^{-4}	2.04×10^{20}	8.03×10^{14}	1.1
2	1003	2.60×10^{-4}	1.57×10^{20}	6.18×10^{14}	0.9
Total oxygen removed		6.39×10^{-4}	3.61×10^{20}	1.42×10^{15}	2.0

[a]Surface area: VPD_{ortho} = 23.18 $m^2 \times g^{-1}$ and VPD_{pyro} = 25.40 $m^2 \times g^{-1}$
[b]The monolayers of oxygen removed are calculated by dividing the oxygen coverage by 7×10^{14} $atom \times cm^{-2}$ – the stoichiometric value of monolayer oxygen coverage.

Catalytic activity

Both samples exhibit catalytic activity with the production of intermediates for *n*-butane selective oxidation to maleic anhydride (MA), *i.e.* butene, butadiene and furan. The temperature profiles of Fig. 5 indicate that by replacement of H_3PO_4 to $H_4P_2O_7$ exhibit minimal influence on the evolution of the catalytic function. VPD_{ortho} developed activity at 674 K (as shown in the onset of furan production in Fig. 6) whereas VPD_{pyro} requires a lower temperature at 588 K. A higher rate of butene production and a lower temperature peak maximum of butene (Fig. 5) shows that VPD_{pyro} gave higher activity as compared to VPD_{ortho}. This is in an agreement with the earlier finding [3]. Total amount of selective products for both catalysts as shown in Table 4 indicate that VPD_{pyro} has a better selectivity.

The most significant observation in the present study is that furan was observed as one of the in-

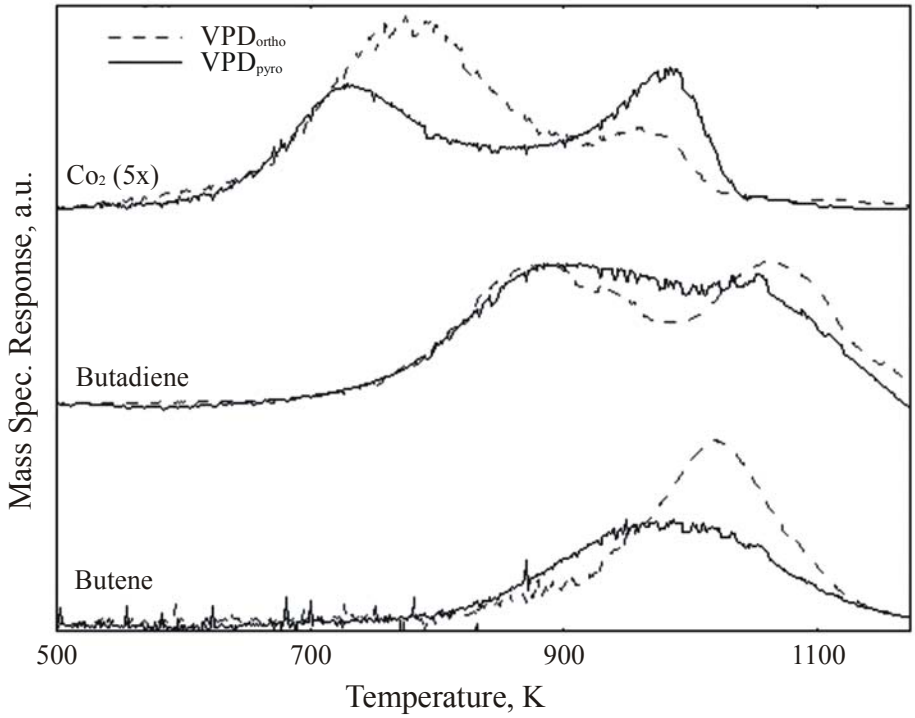

Fig. 5. Production of butene, butadiene, CO_2 by TPRS over the VPD_{ortho} and VPD_{pyro}.

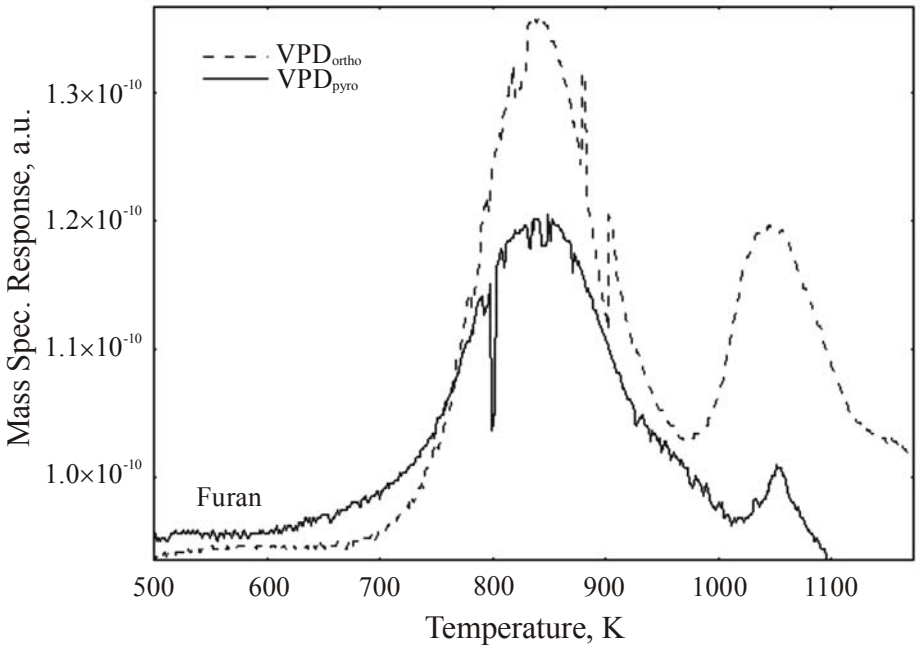

Fig. 6. Production of furan by TPRS of *n*-butane over the VPD_{ortho} and VPD_{pyro}.

Table 4
Percentage of selective and unselective products

Catalysts	But-1-ene	But-1,3-diene	CO	CO_2	Furan
VPD_{ortho}	25.4%	6.08%	66.2%	1.90%	0.62%
VPD_{pyro}	25.4%	6.87%	63.9%	1.90%	0.98%

termediate found for this anaerobic partial oxidation of *n*-butane. This was not observed previously by using the same catalyst prepared using "classical" organic method [10]. The total amounts of CO_2 produced by these two catalysts are similar. However VPD_{ortho} produced higher amount (24% more) of CO_2 at lower temperature peak (783 K) as compared to

VPD_{pyro} which may due to the increment of the V^{5+} oxidation state in the catalyst. Previous study has shown that the presence of V^{5+} phases can decrease the catalytic performances [11,12]. However, according to Abon *et al*. [13], the existence of V^{5+} sites in the catalyst leads to the enhanced catalytic performances for *n*-butane oxidation. The vanadium oxidation state of VPD_{pyro} in this study is 4.18 indicates that the presence of a small amount of V^{5+} is essential for a higher selectivity.

Conclusions

The effect of using $H_4P_2O_7$ in replacement of H_3PO_4 in the synthesised of $(VO)_2P_2O_7$ are:

- A decreased of vanadium oxidation state from 4.26 to 4.18.
- An increasing of the lattice oxygen desorbed thermally.
- The morphology of VPD_{pyro} showed the increasing of isolated platelet for each rosette shape clusters.
- Higher activity and selectivity obtained from *n*-butane oxidation.

References

1. G. Centi, F. Trifiro, J.R. Ebner and V.M. Franchetti, Chem. Rev. 88:55 (1988).
2. G.J. Hutchings, M.T. Sananes, S. Sajip, C.J. Kiely, A. Burrows, I.J. Ellison, J.C. Volta, Catalysis Today 33:161-171 (1997).
3. J.K. Bartley, I.J. Ellison, A. Delimitis, C. J. Kiely, A.Z. Isfahani, C. Rhodes, G.J. Hutchings, Phys. Chem. Chem. Phys. 3:4606-4613 (2001).
4. J.W. Johnson, D.C. Johnson, A.J. Jacobson and J.F. Brody, J. Am. Chem. Soc., 106:8123 (1984).
5. G.J. Hutchings and R. Higgins, J. Catal., 162:153 (1996).
6. G. Poli, I. Resta, O. Ruggeri and F. Trifiro, Appl. Catal., 1:395 (1981).
7. N. Niwa and Y. Murakami, J. Catal. 9:76 (1982).
8. P.H. Klug and L.E. Alexander, X-ray Diffraction Procedures for Polycrystalline and Amorphous Materials. John Wiley & Son, New York., 1974, p. 618.
9. Y.H. Taufiq-Yap, B.H. Sakakini and K.C. Waugh, J. Catal. 46:273-277 (1997).
10. B.H. Sakakini, Y.H. Taufiq-Yap and K.C. Waugh, J. Catal. 189:253 (2000).
11. V.V. Guliants, J.B. Benziger, S. Sundaresan, I.E. Wachs, J.M. Jehng and J.E. Roberts, Catal. Today 28:275 (1996).
12. J.R. Ebner and M. R. Thompson, Catal. Today 16:51 (1993).
13. M. Abon, J.M. Herrmann and J.C. Volta, Catal. Today 71:121-128 (2001).

Received 28 June 2003.